

# Modeling the biomass production of the biofuel crop *Miscanthus x giganteus*, to understand and communicate benefits and risks in cultivation



G.R. Pallipparambil <sup>\*,1</sup>, S. Raghu <sup>2</sup>, R.N. Wiedenmann

319 Agricultural Bldg., Department of Entomology, University of Arkansas, Fayetteville, AR 72701, USA

## ARTICLE INFO

### Article history:

Received 22 June 2013  
Revised 16 April 2015  
Accepted 17 April 2015  
Available online xxxx

### Keywords:

STELLA  
Simulation modeling  
*Miscanthus* productivity  
Systems modeling  
Stakeholders

## ABSTRACT

Bioenergy crop models predict harvestable biomass using known variables, and illustrate key parameters that determine the crop yield. We developed a model, using the systems software STELLA, to provide a conceptual representation of *Miscanthus x giganteus* crop system and understand various parameters and their influence on the growth and loss of harvestable biomass. Using data from four locations, we developed a model and used it to predict yields comparable to reported biomass production from Champaign, IL, thus validating the model structure. Sensitivity analyses of model variables suggested that solar radiation, rainfall, temperature, soil water holding capacity, solar energy interception and conversion efficiency, evapotranspiration, crop coefficient, irrigation and harvest date significantly influenced the predicted harvestable biomass. The flexible STELLA platform also allows the stakeholders to expand and modify the model to incorporate additional variables if required and ultimately enables informed decision-making for bioenergy crop production at any location.

© 2015 International Energy Initiative. Published by Elsevier Inc. All rights reserved.

## Introduction

Novel, non-food, biomass crops (i.e., second generation biofuel crops; “bioenergy crops” hereafter) are increasingly seen as a beneficial carbon-neutral source of energy, and are therefore being promoted and adopted as components of agroecosystems worldwide (Sheppard et al., 2011). Although the increasing costs of fossil fuels are making the uptake of such alternative sources of energy more attractive, there is also increasing attention being paid to the sustainability considerations of cultivating these crops (Raghu et al., 2011; Sheppard et al., 2011). There are significant concerns about the conflicts between biodiversity conservation and the transformation of natural areas and marginal lands into monocultures for the cultivation of bioenergy feedstock (Fargione et al., 2010; Hennenberg et al., 2010). Perhaps of greater concern is the fact that some of the areas earmarked for the development of bioenergy crops are also important agricultural zones for food production (Simmons et al., 2008). The expanding market for bioenergy therefore has the potential to cause transformation of agricultural systems when influenced by the competing demands of food versus fuel production.

Growers typically adapt their production practices to market demands for particular commodities, associated policy and economic incentives, and associated benefits relative to risks and costs; biomass feedstock production is no different in this regard (Jensen et al., 2007; Paulrud and Laitila, 2010). Biomass feedstock production is still in its infancy compared with food-crop agriculture, for which there is a considerable historical scientific and experiential knowledge. Considerable analysis and modeling of the productivity of different bioenergy crops has been undertaken in relation to production location and context, but that work is seldom in a form that a diversity of agricultural stakeholders can probe. The lack of easy understanding of extant models is likely to hinder informed decision-making about the social, economic and environmental sustainability of agricultural practice supporting the cultivation of bioenergy crops (Amigun et al., 2011; Mol, 2007; Selfa et al., 2011).

Our goal with this study was to make some of the basic aspects of the biomass production system accessible to scrutiny by empirical scientists, extension educators and growers (Fig. 1). With the aid of a visual and interactive system-modeling framework, we developed a model for the bioenergy crop *Miscanthus x giganteus* (<sup>3</sup>MxG hereafter). We adapted and expanded published models of this species (Clifton-Brown et al., 2000; Gocic and Trajkovic, 2010; Monteith and Moss, 1977; Price et al., 2004) by integrating agronomic principles and adding modules to enable stakeholders to input information specific to their unique production contexts. The model is developed to input readily available climatic, soil and crop-specific parameters to project

\* Corresponding author at: 1730 Varsity Dr., STE 110, Raleigh, NC 27606, USA. Tel.: +1 919 855 7527; fax: +1 919 513 1114.

E-mail addresses: [grpallip@ncsu.edu](mailto:grpallip@ncsu.edu) (G.R. Pallipparambil), [s.raghu@csiro.au](mailto:s.raghu@csiro.au) (S. Raghu), [rwieden@uark.edu](mailto:rwieden@uark.edu) (R.N. Wiedenmann).

<sup>1</sup> Present address: 1730 Varsity Dr., STE 110, Center for Integrated Pest Management, North Carolina State University, Raleigh, NC 27606, USA.

<sup>2</sup> Present address: CSIRO Biosecurity Flagship, GPO Box 2583, Brisbane, QLD 4001, Australia.

<sup>3</sup> *Miscanthus x giganteus* is abbreviated as MxG.

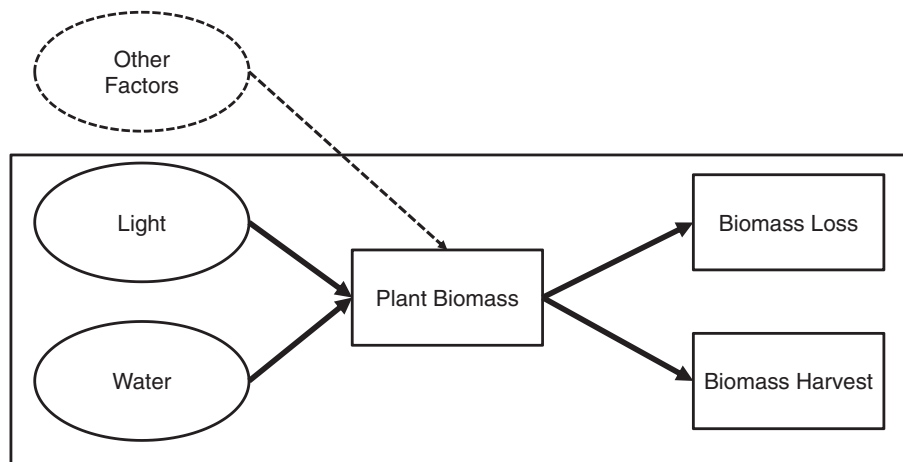


**Fig. 1.** A simplified schematic representation of a biomass production system that we model in this study. The bounds of the model system are indicated within the solid outline and includes the influence of light and water on the production of plant biomass and the harvest and associated losses of plant biomass.

estimates of harvestable biomass of *MxG* in a given location (Fig. 1), grown in any location and under any conditions. We illustrate the value of this model for agricultural stakeholders by simulating the productivity of established stands of *MxG* in five Midwest locations in the US; these locations were chosen as they are being actively promoted as potentially suitable sites for biomass feedstock production by venture capital firms (USDA, 2011). By enabling the users to ‘play’ with different components of the virtual production system and observe their relative influence on harvestable biomass, we demonstrate how more-informed decisions could be made about the cultivation of this species in different geographical contexts.

## Methods

### Model overview

We developed our model using STELLA, a visual system modeling software environment (Research version 9.1.4, iSee Systems, Inc., Lebanon, New Hampshire, U.S.A.). Basic components of a STELLA model include *stocks*, *flows*, *converters* and *connectors*. Stocks (represented as rectangles) characterize components of the model that can be accumulated or depleted, while flows (represented by arrows with valves) characterize activities that lead to accumulation or depletion of stocks. Converters (represented by circles) are parameters in the model that influence flows, while connectors (represented by single-headed arrows) transfer information during simulations from stocks and converters to flows. The bounds/limits of the model are indicated by symbols resembling clouds (for more information on STELLA and its utility see Costanza et al. (1998)).

Our primary objective was to develop a model that would allow a context/location-specific assessment of how the biomass production by an established stand of *MxG* is influenced by solar radiation and water availability – this bounds the system we are investigating. Other factors (e.g., pests or plant diseases) have the potential to influence biomass production, but these factors are often deemed to have relatively minor influences on *MxG* productivity, as it is principally promoted as a bioenergy crop outside of its native range (Heaton et al., 2010a). Therefore our model is limited to the major abiotic influences of light and water availability (Fig. 1).

The major modules of the model include: daily solar radiation of the selected location; efficiency of the plant to intercept and convert solar radiation to dry biomass; the influence of water in the soil available to the plant; and yield losses accrued due to a delay in harvest. The locations at which *MxG* biomass production was simulated for model development included Ashtabula, OH; Aurora, MO; Columbia, MO and

Paragould, AR. These were selected based on these locations being selected by the Biomass Crop Assistance Program (BCAP) for the production of *MxG* by Aloterra Energy LLC and MFA Oil Biomass Company LLC (USDA, 2011). In addition to these four locations, the model was also run using the data from Champaign, IL, for validation.

The model simulates daily biomass production by *MxG* and runs from January 1 (Day 1) to February 28 of the following year (Day 424). There are four phases: the period leading up to the growing season (January to mid-April); the growing season (mid-April to September); senescence and drying down period for standing biomass (October–November); and a harvest window (November–February). The model allows for flexible incorporation of context-specific information on the effects of solar radiation (Fig. 2) and water availability (Fig. 3) on *MxG* dry biomass production and the resultant yield (Fig. 4), to enable stakeholders in the biomass supply-chain to better understand factors in *MxG* cultivation and the associated risks, costs and benefits (Fig. 5).

### Solar radiation and temperature

The influence of solar radiation on biomass production is represented by multiple parameters (Table 1, Fig. 2). Information on solar radiation can be obtained from climate databases (1961–1990) and our model incorporates average daily incident solar radiation (*Daily solar radiation*)<sup>4</sup>.

*Daily mean temperature*, obtained from the national climate database (1981–2010) is translated into *Degree days* that, in turn, influence the development of leaf canopy, represented by *Leaf area index*. The crop leaf area also translates to plant growth through a season, and this information is essential to compute the solar radiation interception efficiency of *MxG* (Fig. 2). The efficiency with which *MxG* plants convert sunlight into biomass (*Radiation use efficiency*) (Table 1) is included as a variable in the model.

In addition to the parameters included in the model, several factors may have a bearing on the conversion of solar radiation into biomass, e.g. variable cloud cover, reduction in solar radiation interception efficiency due to pests and diseases. The modeling framework presented here is flexible enough to incorporate these aspects into the model as and when this information becomes available through ongoing or future research and if it is needed for better predictions.

<sup>4</sup> Here and throughout the manuscript, abbreviations for parameter names/abbreviations are indicated in italics.

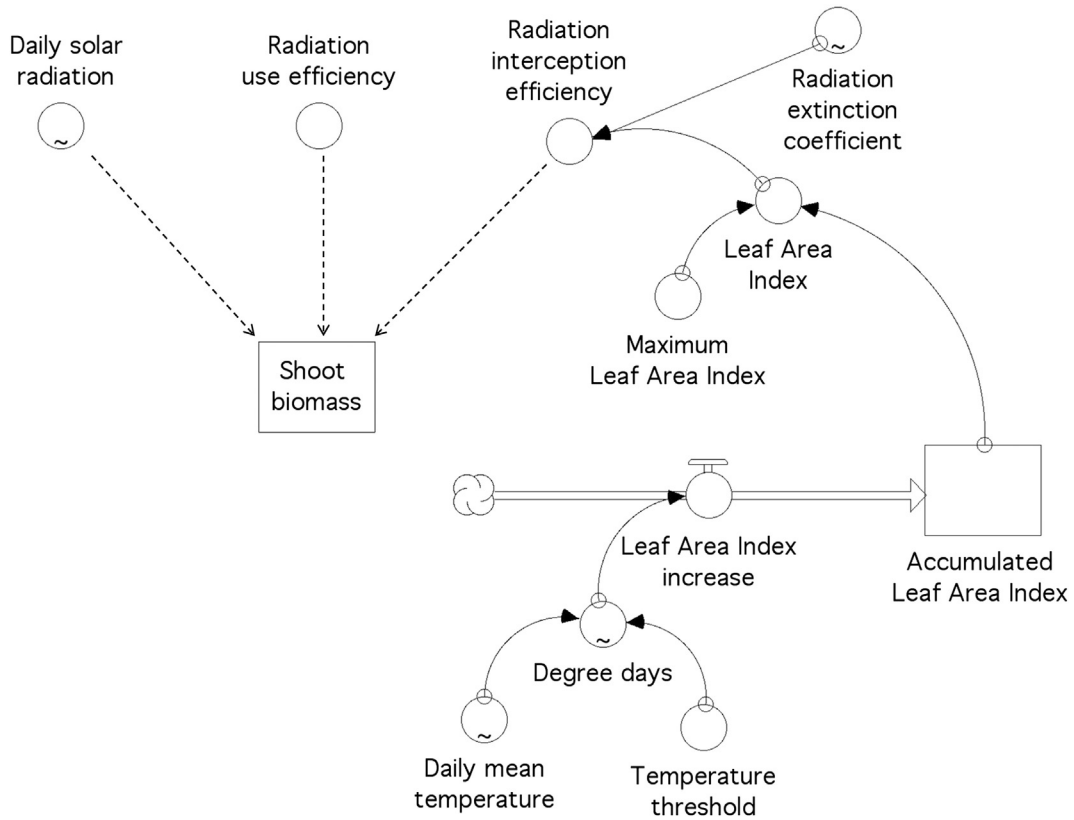


**Fig. 2.** Illustration of how daily solar radiation, and associated parameters like solar radiation use efficiency and solar radiation interception efficiency are incorporated in the model to influence the plant biomass production. The symbols are based on the standard conventions of the STELLA software environment. Rectangles represent stocks/state variables, while arrows with valves represent flows. Circles represent converters and depict parameters in the model; circles with a tilde indicate graphical functions. Arrows represent connectors that transfer information from converters and stocks. See Table 1 for explanations of each of the abbreviations and parameter values.

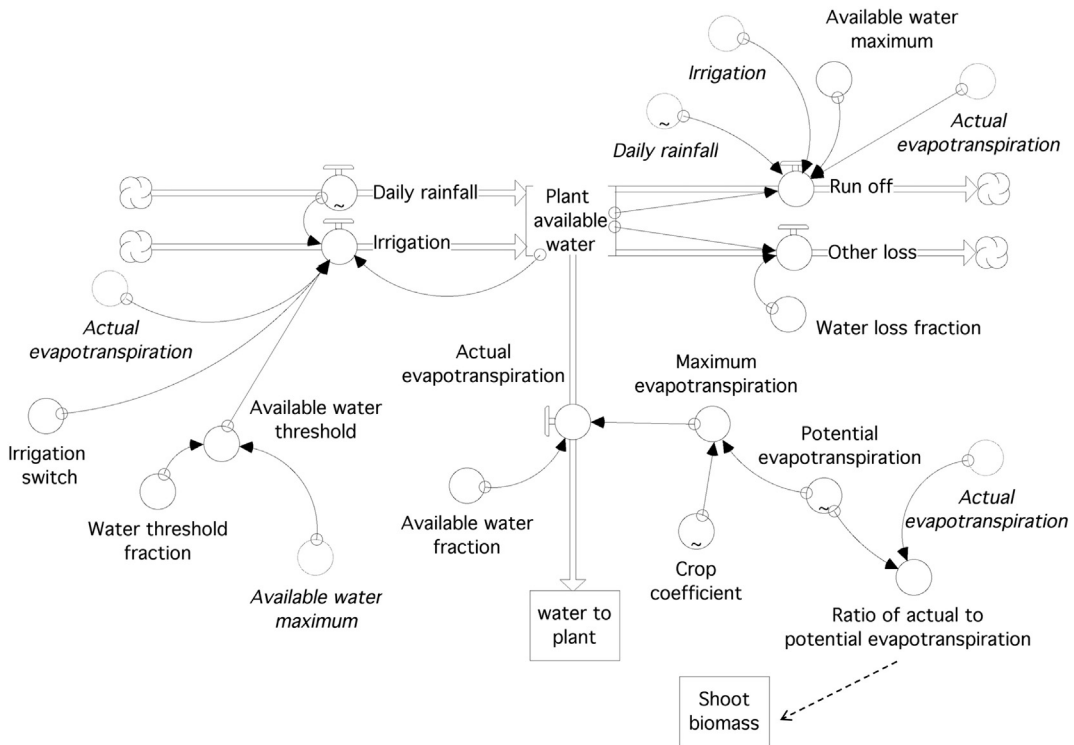


**Fig. 3.** Parameters and relationships that determine water use by MxG in the model. The symbols are based on the standard conventions of the STELLA software environment, as in Fig. 1. See Table 2 for explanations of each of the abbreviations and parameter values.

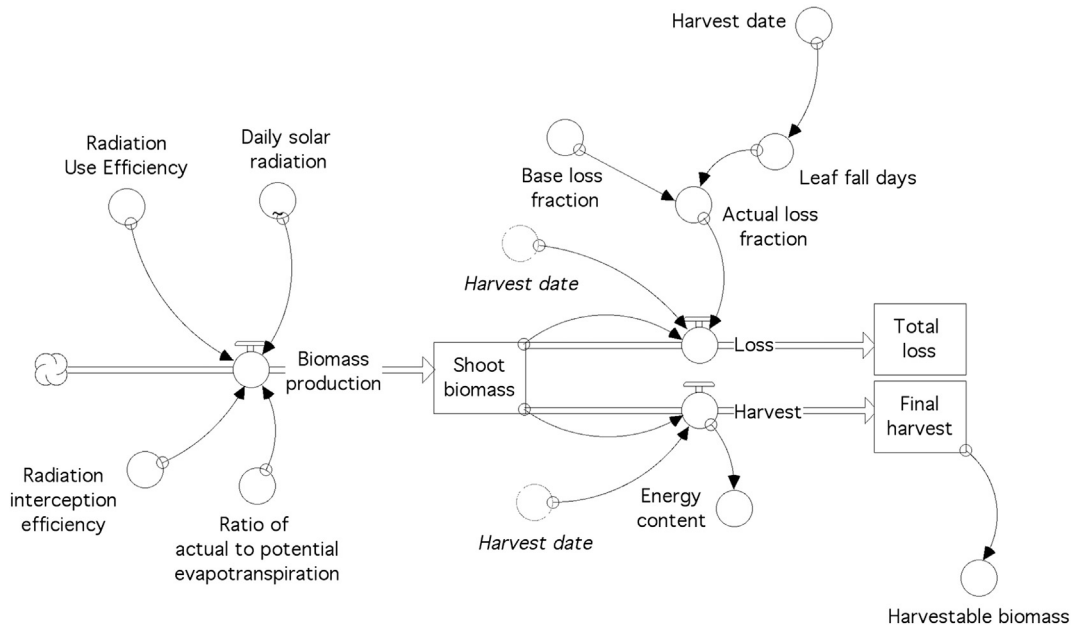


Fig. 4. Schema showing how the model tracks the influence of important factors like solar radiation, temperature, harvest loss and water use on harvestable biomass at the end of a growing season. The symbols are based on the standard conventions of the STELLA software environment, as in Fig. 1. See Table 3 for explanations of each of the abbreviations and parameter values.

Soil water availability and plant water use

The amount of soil water available to the bioenergy crop (plant available water) depends on different parameters associated with the inflow and outflow of water from the soil at any particular point of time (Table 2, Fig. 3). However, much of the plant available water is lost through evapotranspiration. Furthermore, the actual evapotranspiration varies and changes based on the specific crop cultivated (Crop coefficient), available water in the soil (Available water fraction) and growth stage of the plant (Leaf area index) – these interactions

are included in the model. Available water fraction is a linear function of plant available water and the maximum available water content of the soil (Available water maximum; dependent on soil type) (Fig. 3). Actual evapotranspiration also depends on the potential evapotranspiration (Potential evapotranspiration) – a location-specific daily input included in our model. Potential evapotranspiration was estimated based on Gocic and Trajkovic's (2010) software for the calculation of reference evapotranspiration, using limited weather data. This approach utilizes a reduced set Penman–Monteith combination equation that utilizes the following parameters to calculate Potential evapotranspiration: latitude

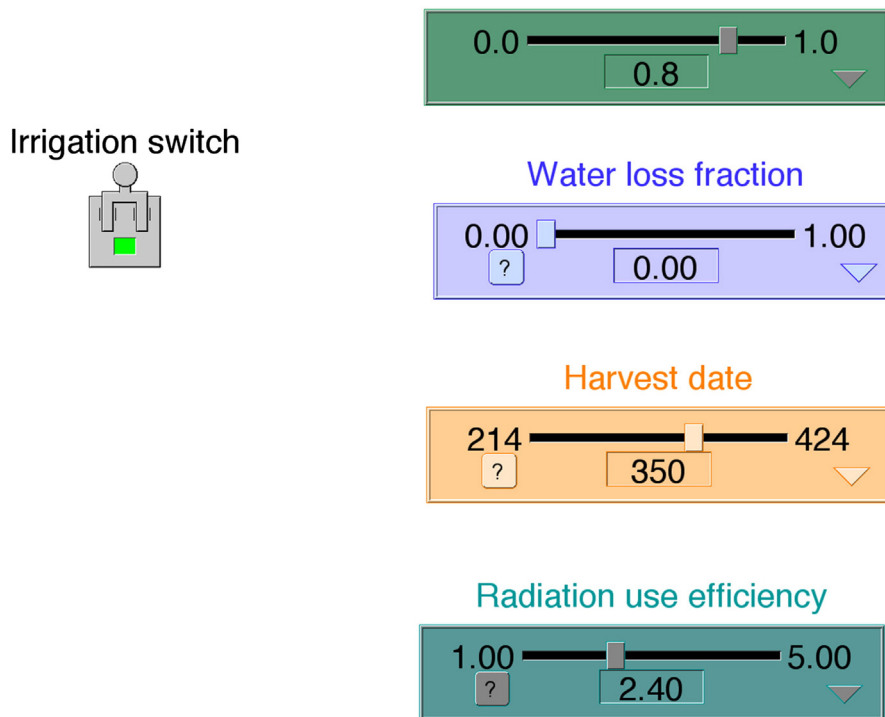


Fig. 5. The model has an easy to use interface allowing the user to change parameters at will. This will aid the model to be used at specific conditions and locations. The symbols are interface icons as it appears on a STELLA model. See Tables 1 to 4 for explanations of the parameters displayed.

**Table 1**Description of parameters for light and their values used in the model. Parameter names/abbreviations are in *italics* (Fig. 2).

Parameter	Description	Default value	Source
<i>Daily solar radiation</i>	Daily incident solar radiation (MJ/m <sup>2</sup> PAR)	Location specific	RReDC-NREL (2012)
<i>Radiation use efficiency</i>	Efficiency with which the intercepted solar radiation is converted to above ground biomass (g/MJ/PAR m <sup>2</sup> )	2.4 (RUE for above ground biomass)	Clifton-Brown et al. (2000)
<i>Daily mean temperature</i>	Average of maximum and minimum daily temperatures (°C)	Location specific	NOAA (2012a b)
<i>Temperature threshold</i>	Base temperature for leaf expansion (°C)	6	Price et al. (2004)
<i>Degree days</i>	Cool degree days with 6 °C as the base temperature for leaf expansion (°D)	<i>Daily mean temperature - Temperature threshold</i> (if <i>mean temperature &gt; threshold</i> ) Else 0	Allen (1976), Baskerville and Emin (1969), Price et al. (2004)
<i>Leaf area index increase<sup>f</sup></i>	Daily Leaf area Index calculated from daily <i>Degree days</i> values	<i>Degree days</i> *0.006	Clifton-Brown and Jones (1999), Price et al. (2004)
<i>Accumulated Leaf area index<sup>s</sup></i>	Daily <i>Leaf area index</i> values accumulated over the growth season	∑ <i>Leaf area index increase</i>	NA
<i>Maximum Leaf area index</i>	<i>Leaf area index</i> when effective crop canopy is assumed to be achieved	5	Price et al. (2004)
<i>Leaf area index</i>	Leaf area index	Minimum ( <i>Accumulated LAI</i> , <i>Presumed max LAI</i> )	NA
<i>Radiation extinction coefficient</i>	Extinction coefficient for solar radiation in plant canopies (Varies with plant phenology)	0.56–0.68	Clifton-Brown et al. (2000), Price et al. (2004), Zub and Brancourt-Hulmel, (2010)
<i>Radiation interception efficiency</i>	Solar radiation interception efficiency of the canopy (dimensionless)	$1 - e^{-K \cdot LAI}$ , where K = radiation extinction coefficient and LAI = leaf area index	Clifton-Brown et al. (2000), Price et al. (2004)

s = Stock; f = Flow.

and elevation (m) of the location; daily maximum and minimum temperatures; solar radiation (MJm<sup>-2</sup> day<sup>-1</sup>); wind speed (ms<sup>-1</sup>); and dew point temperature (°C). In addition to evapotranspiration, water available in the soil may also be lost as surface *Run off* and sub-surface deep percolation (*Other loss*), both of which are factored into the model. The value of *Other loss* is influenced by a second parameter, *water loss fraction*, and its default value is set as zero, limiting the default water loss in the model to runoff and evapotranspiration.

Rainfall is the major contributor to *Plant available water*. Precipitation (*Daily rainfall*) data can be obtained from weather stations nearest to the location of interest. In our model, the rainfall data for each location was selected for the 30-year period from 1980 to 2010 and the median, below median (first quartile) and above median (third quartile) rainfall years were calculated to simulate different rainfall scenarios. In addition to this input, any deficit from the optimal water requirements for the bioenergy crop can also be made up by irrigation (*Irrigation*) in the model.

**Table 2**

Description of parameters for water and their values used in the model (Fig. 3).

Parameter	Description	Default value	Source
<i>Plant available water<sup>s</sup></i>	The amount of soil water available to the plant (mm)	0.5* <i>Available water maximum</i>	NA
<i>Daily rainfall<sup>f</sup></i>	Daily precipitation (mm)	Location specific, daily value for a specific year (1999–2010)	NOAA (2012b)
<i>Available water maximum</i>	Maximum plant available water in the soil (mm)	Location specific	Rawls et al. (1992); USDA-NRCS (2012)
<i>Water threshold fraction</i>	Parameter to allow the modification of <i>Available water maximum</i> for irrigation requirement	0.8 (user can modify based on the preferred minimum <i>Plant available water</i> )	NA
<i>Available water threshold</i>	If the plant available water drops below this level, irrigation commences (mm)	<i>Available water threshold</i> * <i>Water threshold fraction</i>	NA
<i>Irrigation<sup>f</sup></i>	Supplementary water input to the plant available water when rainfall is low		NA
<i>Irrigation switch</i>	Allows the model to supplement input water with irrigation	1/0	NA
<i>Total irrigation<sup>s</sup></i>	Total amount of water that is used for irrigation in a growing season (mm)	Initial value = 0	NA
<i>Potential evapotranspiration</i>	Daily average potential evapotranspiration calculated using a modified Penman–Monteith combination (FAO-56 PM) equation (mm)	Location-specific	Gocic and Trajkovic (2010)
<i>Crop coefficient</i>	Ratio of the total evaporation from the crop to the potential evapotranspiration (varies with season)	0.48–1.15	Beale et al. (1999)
<i>Maximum evapotranspiration</i>	Maximum evapotranspiration for a crop when water is unlimited (mm)	<i>Potential evapotranspiration</i> * <i>Crop coefficient</i>	Allen (1998)
<i>Available water fraction</i>	A fraction that increases linearly with plant available water	0–1	NA
<i>Actual evapotranspiration<sup>f</sup></i>	Actual evapotranspiration is <i>Maximum evapotranspiration</i> when water is limited (mm)	<i>Maximum evapotranspiration</i> * <i>Available water fraction</i> during the growth period	NA
<i>Water to plant<sup>s</sup></i>	Total amount of water available to the plant through <i>ETa</i> in a season (mm)	Initial value = 0	
<i>Ratio of actual to potential evapotranspiration</i>	This fraction of evapotranspiration is variable throughout the growing season	0–1	Clifton-Brown et al. (2004), Heaton et al. (2010a, 2010b), Price et al. (2004)
<i>Run off<sup>f</sup></i>	Water removal from the plant available water as run off from the soil	$f$ ( <i>Plant available water</i> , <i>actual evapotranspiration</i> , <i>Rainfall</i> , <i>Irrigation</i> ). Value between 0– <i>Available water maximum</i> .	NA
<i>Other loss<sup>f</sup></i>	Water removal from the plant available water other than <i>Run off</i> . Eg. deep drainage	0	Arnold (2011), Sammis et al. (1982)
<i>Water loss fraction</i>	Fraction of water that is lost other than <i>Run off</i> from the <i>Plant available water</i>	0	
<i>Water lost<sup>s</sup></i>	Total amount of water that <i>Run off</i> in a growing season (mm)	Initial value = 0	NA

s = Stock; f = Flow.

The amount of soil moisture also depends on the type of soil, depth of different soil layers and their ability to store water. This parameter varies by location, and understanding the influence of soil type on biomass production allows us to select sites for optimal crop growth. Soil type and thickness of different layers can be used to compute the available water content (*Available water maximum*) in a specific location using the equation  $\sum[(\text{Water content at field moisture capacity} - \text{Water content at permanent wilting point}) \times \text{thickness of horizon}]$  for each soil layer for a depth of 150 cm (Rawls et al., 1992). For each of the five locations in this study, we calculate *Available water maximum* by (a) identifying the soil type at multiple sites in a location of interest (e.g. Ashtabula County) (b) calculating *Available water maximum* for each of the different sites at the location of interest and based on this, (c) calculating an average *Available water maximum* for the entire county or location of interest and (d) using this average as the *Available water maximum* for the model location. Model users can use location-specific information on *Available water maximum* if available.

#### Plant biomass production, loss & harvest

In general, plant growth depends on parameters like water availability, temperature, and the type of crop. In our model, biomass production of MxG depends on water, solar radiation and assumes a specific planting density, growing season and harvest date based on common agronomic practices for MxG and scientific evidence. The planting density of MxG used in the model is 1.5 plants  $\text{m}^{-2}$ , the rate recommended by current agronomic practice (Bullard and Nixon, 1999; Price et al., 2004; USDA, 2011). The growing season of MxG starts with crop emergence in April and proceeds to attain maximum biomass in August, after which a daily leaf loss may occur until the date of harvest. The harvest date (*Harvest date*) may vary and is dependent on the grower's preference to allow the crop to senesce and dry down to the specifications for feedstock or to facilitate nutrient translocation to roots. However, delaying harvest can also result in leaf loss, reducing the total harvestable biomass. By providing the date of harvest as an input (default *Harvest date* is December 15), the model will calculate the biomass lost due to this delay (*Loss*). Our model assumes that there is a steady reduction of 0.25% daily yield from September to December, with a maximum possible yield loss of 30% by the end of December (Clifton-Brown et al., 2004; Heaton et al., 2010b). Based on the harvest date and after accounting for the daily losses, the model computes the daily biomass at final harvest (*Final harvest* ( $\text{gm}^{-2}$ )) that can be converted to *Harvestable biomass* ( $\text{t ha}^{-1}$ )) (Table 3, Fig. 4).

**Table 3**  
Description of parameters for biomass production and removal, and their values used in the model (Fig. 4).

Parameter	Description	Default value	Source
<i>Shoot biomass</i> <sup>s</sup>	The accumulated above ground biomass of the plant ( $\text{g/m}^2$ )	Calculated from other parameters	NA
<i>Biomass production</i> <sup>f</sup>	Biomass produced per day ( $\text{g/m}^2$ )	$\text{Solar radiation} * \text{Ec variation} * \text{Ei} * \text{ETap ratio}$	Monteith and Moss (1977), Price et al. (2004)
<i>Harvest date</i>	Nth day of harvest. Value can be selected from August 1st (214) of current year to February 28th (424) of the next year. Used here to calculate <i>Leaf fall days</i>	350 (December 15)	NA
<i>Leaf fall days</i>	Number of days until <i>Harvest date</i> after the crop has attained maximum biomass	<i>Harvest date</i> – 240	NA
<i>Base loss fraction</i>	Proportion of reduction in daily yield for each <i>Leaf fall day</i>	0.0025	Clifton-Brown et al. (2004), Heaton et al. (2010)
<i>Actual loss fraction</i>	Proportion of reduction in total yield	0.28	
<i>Loss</i> <sup>f</sup>	Daily loss of biomass until the harvest date ( $\text{g/m}^2$ )		
	$\text{Shoot\_biomass} * \text{Actual\_loss\_fraction}$		
<i>Total loss</i> <sup>s</sup>	Accumulated total loss for the season ( $\text{g/m}^2$ )	$\sum \text{Loss}$	
<i>Harvest</i> <sup>f</sup>	Daily harvested biomass ( $\text{g/m}^2$ )	$\text{Shoot biomass at Harvest date}$	
<i>Final harvest</i> <sup>s</sup>	Total harvested aboveground biomass for the season ( $\text{g/m}^2$ )	$\sum \text{Harvest}$	
<i>Harvestable biomass</i>	Unit conversion of <i>Final harvest</i> to tons/ha	( <i>Final harvest</i> * 0.01)	
<i>Energy content</i>	Energy content of the harvested <i>Miscanthus X giganteus</i> crop ( $\text{MJ/m}^2$ )	( <i>Final Harvest</i> / 1000) * 18.4	Beale et al. (1996), Beale and Long (1995), Jones and Walsh (2001)

s = Stock; f = Flow.

#### Parameters available for user control

Several parameters in the model are specific to each location and, therefore, are imported from a spreadsheet for that location. These parameters include *Daily solar radiation*, *Daily mean temperature*, *Daily rainfall*, *Available water maximum* and *Potential evapotranspiration* (Figs. 2, 3). However, the user can choose to vary several other parameters available at the model user interface (Fig. 5); this includes *Water threshold fraction*, *Water loss fraction*, *Harvest date* and *Radiation use efficiency*.

For example, an irrigation event is set to trigger at a default value of *Water threshold fraction* = 0.8 or lower i.e., if the soil moisture drops below 80% of the *Available water maximum*, an irrigation event is triggered. If the user can tolerate a higher water deficit, the *Water threshold fraction* value can be lowered at the user interface of the model. Our calculations do not include variations in topography at each location and, therefore, consider the planted area to be of uniform slope. However, any percent increase in water loss due to change in slope could be adjusted in a parameter, *water loss fraction*, which is available for the user at the model interface.

Because *Radiation use efficiency* may differ among crops, it is provided as a variable available for the user to modify on the interface. This will aid in the modeling of different bioenergy crops using a standard model framework. Another parameter available on the user interface is *Harvest date*. Changing this parameter varies the amount of leaf loss accrued per day until the date of harvest, which may be anytime between August and March of the following year.

#### Model validation

The model was run for Champaign, IL, USA to validate against existing yield data available for the location. Our model used precipitation, daily solar radiation, plant available water based on soil type, potential evapotranspiration and average daily temperature at Champaign, IL, as inputs to predict the yield (Table 4). The average predicted biomass output of different locations ( $\sim 31.5 \text{ t ha}^{-1}$ ) from our model is comparable to the actual yield data ( $25\text{--}35 \text{ t ha}^{-1}$ ) reported from multiyear field trials in Urbana-Champaign (Arundale et al., 2014; Dohleman et al., 2012; Heaton et al., 2008), which suggests that our model captures the core aspects of the physiology of biomass accumulation in MxG.

#### Sensitivity analyses

A sensitivity analysis enables the user to determine responses of key model outputs (e.g., harvestable biomass) to variations in selected

**Table 4**

Predicted harvestable biomass yield during a below median, median or above median rainfall year for the locations Ashtabula, OH; Champaign, IL; Aurora, MO; Columbia, MO and Paragould, AR.

Location	Rainfall	Yield (t/ha)	
		No irrigation	With irrigation
Ashtabula	Below median	23.7	26.1
	Median	25.5	26.5
	Above median	24.5	27.1
Champaign	Below median	31.9	34.0
	Median	30.2	33.6
	Above median	30.0	33.3
Aurora	Below median	32.9	39.1
	Median	33.4	39.6
	Above median	38.5	40.6
Columbia	Below median	35.8	38.7
	Median	34.7	38.0
	Above median	34.3	38.2
Paragould	Below median	36.1	41.6
	Median	33.8	41.1
	Above median	36.0	41.1

parameters for each of the locations of interest. Such an approach enables model users to investigate the relative importance of each parameter to biomass production in different production contexts. A sensitivity analysis for the key model parameters (*daily solar radiation, Radiation use efficiency, crop coefficient, Leaf area index, Daily mean temperature, harvest date, base loss fraction, Available water maximum, daily rainfall, water loss fraction, Available water fraction and Potential evapotranspiration*) was conducted for each of the five locations to examine if the trends in sensitivity were location-dependent. The sensitivity of harvestable yield to a given parameter in the model was evaluated by varying the parameter value between 50 and 200% of its default value in the model, while holding all other parameters at their default values (Tables 1–3). For *water loss fraction*, we varied values from 0 to 50%. Rainfall was held at the median rainfall for each location, and the sensitivity of yield was evaluated both with and without irrigation. The parameters to which yield was most sensitive were identified by the use of comparative graphs.

The rank order of the locations in terms of their suitability for *MxG* production does not change markedly under any of the range of parameters simulated as part of the sensitivity analyses. Biomass yield ranged from 20 to 40 t ha<sup>-1</sup> across most of the simulations. In the absence of irrigation, solar radiation appears to have the greatest influence on yield (Fig. 6A), while the potential for subsurface water loss appears to have the strongest negative influence (Fig. 6K). The loss of leaves prior to harvest (Fig. 6E) and evapotranspiration (Fig. 6I) has strong negative linear effects on yield. Leaf area index, rainfall, plant available water content in the soil and temperature all appear to have threshold effects on yield, with only the lower range (less than about 1.0 of the parameter range on X-axis) of parameter estimates resulting in increases to yield (Figs. 6C, F, G, J). Varying *Water threshold fraction* has no influence on yield; this is unsurprising in the absence of irrigation, as this parameter is a trigger for irrigation. *Harvest date* has an interesting breakpoint effect with a slight delay beyond the default (December 15) harvest date having the highest yield across all locations; harvest before or after results in diminished yields (Fig. 6D). This suggests that timing of the harvest is likely to be critical to optimize yield.

The patterns in sensitivity of yield in the presence of irrigation largely mirror those in the absence of irrigation (Figs. 6, 7). The notable exception to this trend is the role of *Water threshold fraction* that had a threshold effect in the absence of irrigation (Figs. 6H, 7H).

Given the aim of the model (i.e. provision of a conceptual representation of the *Miscanthus x giganteus* crop system a learning tool to facilitate stakeholders to engage with the decision-making process on sustainable biomass production), more sophisticated sensitivity

analyses (Saltelli and Annoni, 2010) were not attempted as part of this study.

#### Model use

Given the ability of the model to reasonably predict the yield of *MxG* and the trends in sensitivity, it is possible to use the model to examine the production of *MxG* in different locations, and under different rainfall and irrigation scenarios. Harvestable biomass yield predicted was different for each of the five locations of interest and this varied based on irrigation and rainfall (Table 4). In the absence of irrigation, increasing rainfall did not automatically result in increased yields across all locations; only Aurora fitted this trend (Table 4). At Ashtabula, the median rainfall scenario resulted in the best yield; in contrast, in Champaign and Columbia, the below-median rainfall scenario gave the highest yield. Intriguingly, at Paragould, the median rainfall scenario had the lowest yield; this may have been due to the clustered distribution of rainfall days for the median rainfall year at this location. In the presence of irrigation, yields stabilized to be relatively similar across all the three rainfall scenarios across all locations (Table 4).

In the absence of irrigation, in general, Paragould, AR and Columbia, MO showed a similarly high yield, followed by Aurora, MO, Champaign, IL and Ashtabula, OH (Table 4). In the presence of irrigation, Columbia had the highest biomass yield, followed by Aurora, Paragould, Champaign and Ashtabula (Table 4).

#### Discussion

Our goal with the model was to provide a tool to enable different stakeholders to understand the potential to produce the bioenergy crop *MxG* in different locations. The model was developed to accept input of readily available climatic, soil and crop-specific information and, by their integration using agronomic principles, project estimates of harvestable biomass of *MxG* in a given location, and under varying scenarios.

Several models exist for predicting the harvestable biomass of bioenergy crops. MISCANMOD/MISCANFOR was developed based on some of the same principles as our model (Monteith and Moss, 1977); a semi-mechanistic, plant-production model, WIMOVAC (Beale and Long, 1995), was adapted specifically for *MxG* (Miguez et al., 2009). Though the predictions of yield of *MxG* in Champaign matched that predicted by these other production models and field data for this species, our relative predictions of biomass do not precisely match the predicted yields presented in the USDA report for the Biomass Crop Assistance Program (USDA, 2011). This difference is not altogether surprising, given that our model only incorporates the influences of light and water availability. Other factors – e.g., soil fertility – are also critical determinants of biomass yield, and incorporating those into our model may enhance the precision of estimates. Soil fertility can either be incorporated by including detailed information on influences of soil fertility on *MxG* yields or using proxies for relative fertility of different locations. For example, relative yields of another widespread grass crop with a similar C<sub>4</sub> carbon fixation mechanism (e.g., corn) grown in each of the locations may be used to develop an index that serves as a proxy for soil fertility; this index could be used to weigh *MxG* growth rates in each of the production locations.

Other aspects that are missing from most present models of *MxG* are those relating to the role of pests and diseases in limiting yield. Though exotic to the US, *MxG* may influence and may be influenced by, the abundance of insect herbivores and plant pathogens in agroecosystems (Bradshaw et al., 2010; Nabity et al., 2011; Prasifka et al., 2011; Prasifka, 2011; Prasifka et al., 2009; Spencer and Raghu, 2009). As in the above case of soil fertility, location-specific information on the different pest pressures likely to impact *MxG* yield can be incorporated into our modeling approach if the model does not provide reasonable predictions with the current parameters.

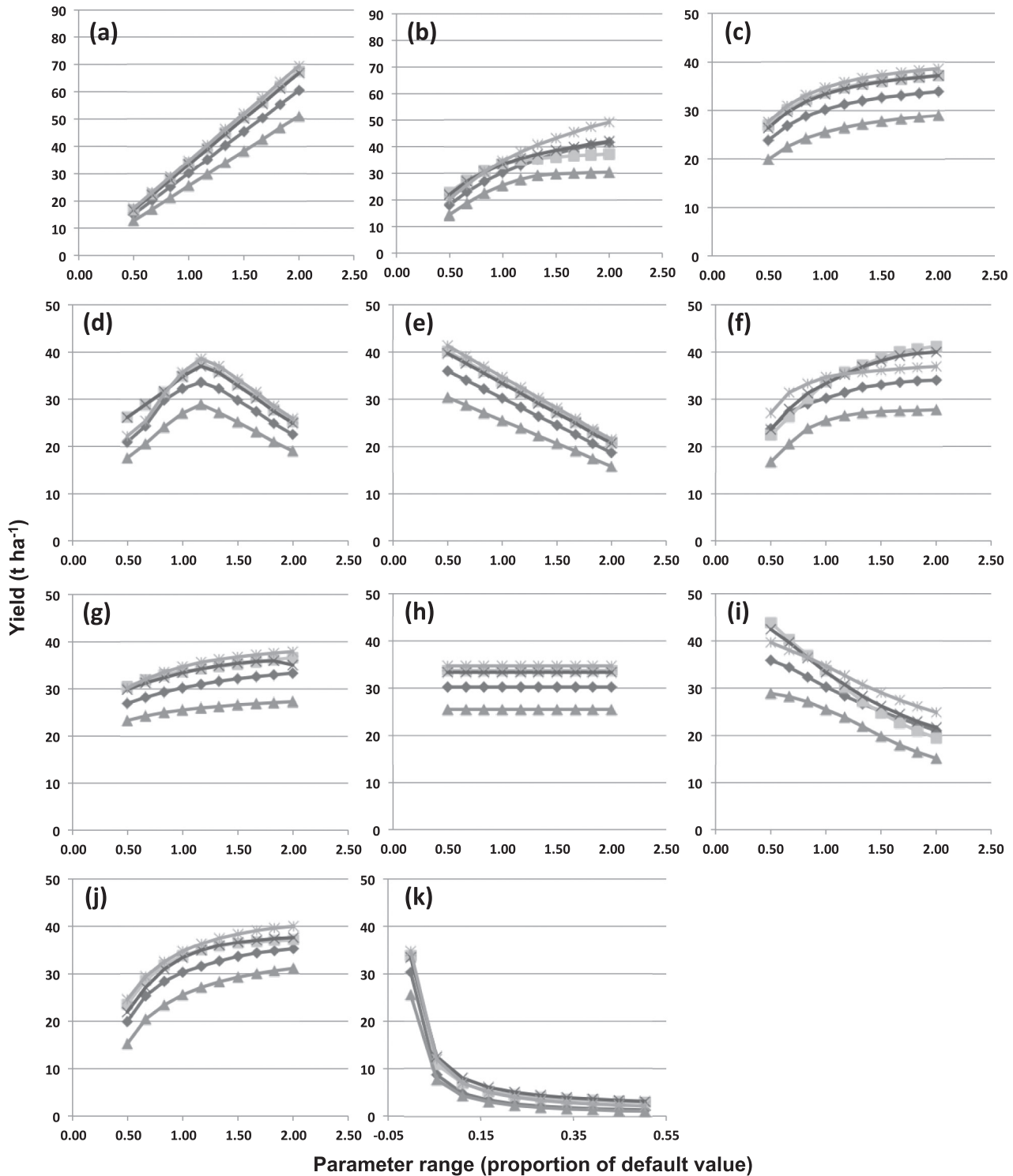


**Fig. 6.** Sensitivity analyses showing the impacts on yield ( $\text{t ha}^{-1}$ ) of the bioenergy crop *Miscanthus x giganteus* from varying the key parameters (a) Solar radiation,  $E_c$ , (b) Crop coefficient, (c) LAI, (d) Harvest date, (e) Base loss fraction, (f) Rainfall, (g) AWC, (h) AWCfr, (i)  $ET_p$ , (j)  $T_m$  and (k) Water loss fraction in five different production locations, in the presence of irrigation. Production locations are Champaign, IL (◆), Paragould, AR (■), Ashtabula, OH (▲), Aurora, MO (×) and Columbia, MO (\*). There is only one set of graphs for Solar radiation and  $E_c$  as their influence on yield is identical. Note differences in the y-axis scale for A and B, and the x-axis for K; see Tables 1 to 3 for definitions and default values of parameters.

## Conclusions

Our modeling framework using STELLA can be used to identify suitable locations to grow biofuel crops such as *MxG*, and to identify sensitive parameters that may influence biomass production at these locations. Although our model is amenable to refinements to

enhance precision, an important caveat is that the goal of our model is not necessarily prediction of yield with precision, but to demonstrate the utility of such system modeling approaches in examining the underlying causes of system dynamics, and as a tool to engage stakeholders in outreach and extension activities around sustainable biomass production. Most of the other models that simulate

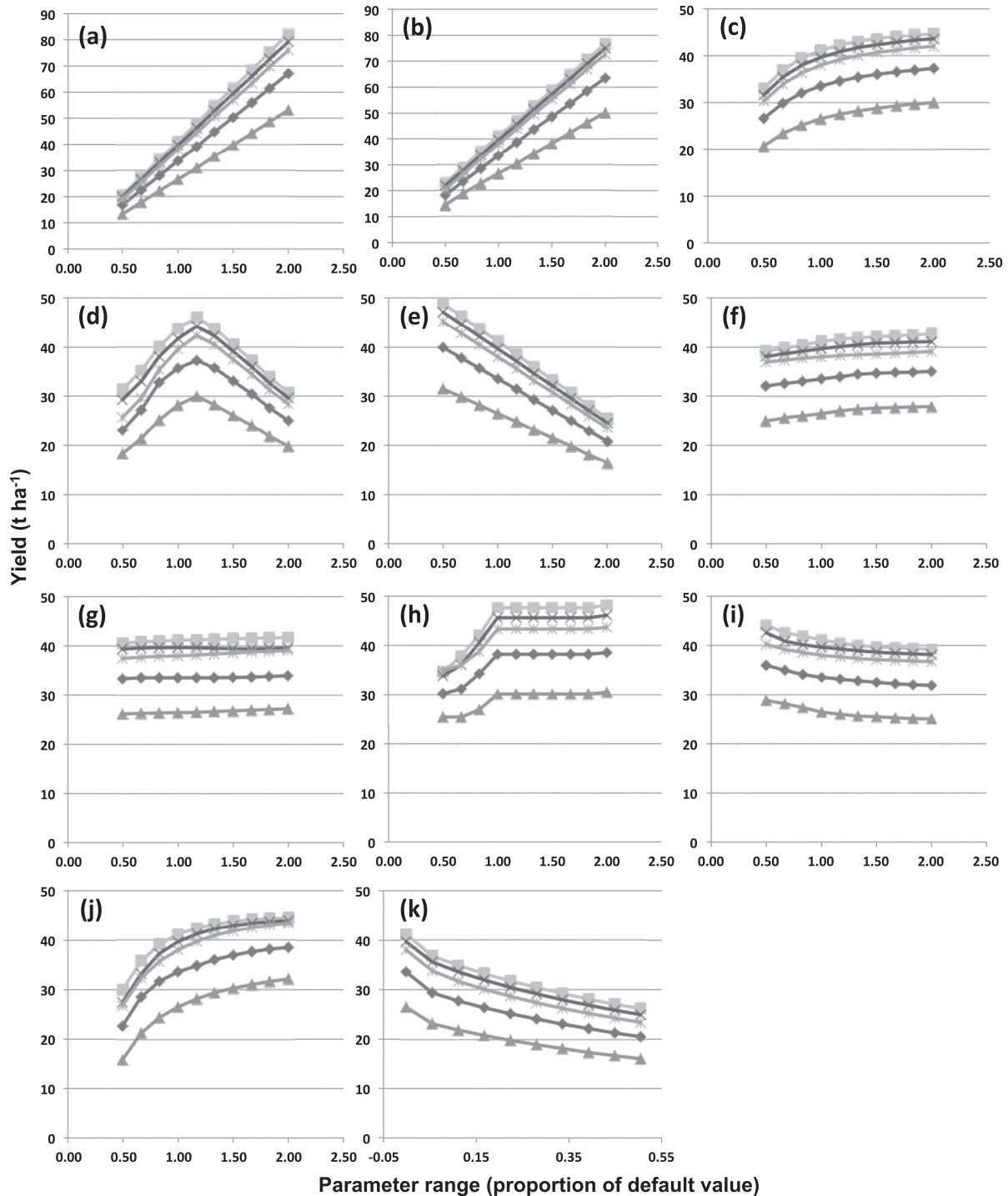


**Fig. 7.** Sensitivity analyses showing the impacts on yield ( $\text{t ha}^{-1}$ ) of the bioenergy crop *Miscanthus x giganteus* from varying the key parameters ((a) Solar radiation,  $E_c$ , (b) Crop coefficient, (c) LAI, (d) Harvest date, (e) Base loss fraction, (f) Rainfall, (g) AWC, (h) AWC fr, (i) ETp, (j) Tm and (k) Water loss fraction) in five different production locations, in the absence of irrigation. Production locations are Champaign, IL (◆), Paragould, AR (■), Ashtabula, OH (▲), Aurora, MO (×) and Columbia, MO (\*). There is only one set of graphs for Solar radiation and  $E_c$  as their influence on yield is identical. Note differences in the y-axis scale for A and B, and the x-axis for K; see Tables 1 to 3 for definitions and default values of parameters.

biomass production do not allow easy examination of model components and assumptions by users other than bioenergy researchers; filling this important gap for outreach and extension was the primary motivation for this study. Our model explains each parameter, visually depicts the connection between the parameters, and allows associating contribution of the parameters towards the accumulation of biomass. To determine the potential biomass productivity at a given location, the user may only need to input data for the

location-specific parameters listed in Tables 1–3. For example, climate data for a specific location are publicly available from the National Oceanic and Atmospheric Administration (NOAA). The NOAA data from the excel sheet can be directly imported into the model for obtaining location-specific biomass estimates. At present, the model is available as a standalone STELLA file; however, we will also examine potential integration of the model in websites for easy access to the stakeholders.

## Acknowledgements

This project was supported by Award DE-FG36-08G088036, “MidSouth/Southeast BioEnergy Consortium,” from the US Department of Energy. The complete model is available on request from the authors.

## References

- Allen JC. A modified sine wave method for calculating degree days. *Environ Entomol* 1976;5:388–96.
- Allen RG. Crop evapotranspiration : guidelines for computing crop water requirements. Rome: Food and Agriculture Organization of the United Nations; 1998.
- Amigun B, Musango JK, Brent AC. Community perspectives on the introduction of biodiesel production in the Eastern Cape Province of South Africa. *Energy* 2011;36:2502–8.
- Arnold LR. Estimates of deep-percolation return flow beneath a flood- and a sprinkler-irrigated site in Weld County, Colorado, 2008–2009. Scientific Investigations Report US Department of the Interior US Geological Survey; 2011.
- Arundale RA, Dohleman FG, Heaton EA, Mcgrath JM, Voigt TB, Long SP. Yields of *Miscanthus x giganteus* and *Panicum virgatum* decline with stand age in the Midwestern USA. *GCB Bioenergy* 2014;6:1–13.
- Baskerville GL, Emin P. Rapid estimation of heat accumulation from maximum and minimum temperatures. *Ecology* 1969;50:514–7.
- Beale CV, Long SP. Can perennial C-4 grasses attain high efficiencies of radiant energy-conversion in cool climates. *Plant Cell Environ* 1995;18:641–50.
- Beale CV, Bint DA, Long SP. Leaf photosynthesis in the C-4-grass *Miscanthus x giganteus*, growing in the cool temperate climate of southern England. *J Exp Bot* 1996;47:267–73.
- Beale CV, Morison JIL, Long SP. Water use efficiency of C-4 perennial grasses in a temperate climate. *Agr Forest Meteorol* 1999;96:103–15.
- Bradshaw JD, Prasifka JR, Steffey KL, Gray ME. First report of field populations of two potential aphid pests of the bioenergy crop *Miscanthus x giganteus*. *Fla Entomol* 2010;93:135–7.
- Bullard MJ, Nixon PML. *M. x giganteus* agronomy for fuel and industrial uses. Project report (NF0403) for MAFF; 1999.
- Clifton-Brown JC, Jones MB. Alteration of transpiration rate, by changing air vapour pressure deficit, influences leaf extension rate transiently in *Miscanthus*. *J Exp Bot* 1999;50:1393–401.
- Clifton-Brown JC, Neilson B, Lewandowski I, Jones MB. The modelled productivity of *Miscanthus x giganteus* (GREEF et DEU) in Ireland. *Ind Crop Prod* 2000;12:97–109.
- Clifton-Brown JC, Stampfl PF, Jones MB. *Miscanthus* biomass production for energy in Europe and its potential contribution to decreasing fossil fuel carbon emissions. *Glob Chang Biol* 2004;10:509–18.
- Costanza R, Duplisea D, Kautsky U. Ecological modelling and economic systems with STELLA — introduction. *Ecol Model* 1998;110:1–4.
- Dohleman FG, Heaton EA, Arundale RA, Long SP. Seasonal dynamics of above-and below-ground biomass and nitrogen partitioning in *Miscanthus x giganteus* and *Panicum virgatum* across three growing seasons. *GCB Bioenergy* 2012;4:534–44.
- Fargione JE, Plevin RJ, Hill JD. The ecological impact of biofuels. *Annu Rev Ecol Syst* 2010;41:351–77.
- Gocic M, Trajkovic S. Software for estimating reference evapotranspiration using limited weather data. *Comput Electron Agric* 2010;71:158–62.
- Heaton EA, Dohleman FG, Long SP. Meeting US biofuel goals with less land: the potential of *Miscanthus*. *Glob Chang Biol* 2008;14:2000–14.
- Heaton E, Moore KG, Salas-Fernandez M, Hartzler B, Liebman M, Barnhart S. Giant miscanthus for biomass production. In: University IS, editor. AG201 biomass: *Miscanthus* factsheet: factsheet; 2010a.
- Heaton EA, Dohleman FG, Miguez AF, Juvik JA, Widholm J, Mcissac GF, et al. *Miscanthus*: a promising biomass crop. *Adv Bot Res* 2010b;56:75–137.
- Hennenberg KJ, Dragisic C, Hays S, Hewson J, Semroc B, Savy C, et al. Sustainability of bioenergy: do existing standards meet protection needs for biodiversity. *Conserv Biol* 2010;24:412–23.
- Jensen K, Clark CD, Ellis P, English B, Menard J, Walsh M, et al. Farmer willingness to grow switchgrass for energy production. *Biomass Bioenergy* 2007;31:773–81.
- Jones MB, Walsh M. *Miscanthus* — for energy and fibre. London: James and James (Science Publishers); 2001.
- Miguez FE, Zhu XG, Humphries S, Bollero GA, Long SP. A semimechanistic model predicting the growth and production of the bioenergy crop *Miscanthus x giganteus*: description, parameterization and validation. *GCB Bioenergy* 2009;1:282–96.
- Mol APJ. Boundless biofuels? Between environmental sustainability and vulnerability. *Sociol Rural* 2007;47:297–315.
- Monteith JL, Moss CJ. Climate and the efficiency of crop production in Britain. *Philos Trans R Soc Lond B Biol Sci* 1977;281:277–94.
- Nabity PD, Zangerl AR, Berenbaum MR, DeLucia EH. Bioenergy crops *Miscanthus x giganteus* and *Panicum virgatum* reduce growth and survivorship of *Spodoptera frugiperda* (Lepidoptera: Noctuidae). *J Econ Entomol* 2011;104:459–64.
- NOAA. Monthly and seasonal color outlook maps. National Oceanic and Atmospheric Administration, US Department of Commerce; 2012a [[http://www.cpc.ncep.noaa.gov/products/predictions/multi\\_season/13\\_seasonal\\_outlooks/color/churchill.php](http://www.cpc.ncep.noaa.gov/products/predictions/multi_season/13_seasonal_outlooks/color/churchill.php)].
- NOAA. Online weather data from the National Weather Service Forecast Office. National Oceanic and Atmospheric Administration, US Department of Commerce; 2012b [<http://www.nws.noaa.gov/climate/xmacis.php?wfo = CLE>].
- Paulrud S, Laitila T. Farmers' attitudes about growing energy crops: a choice experiment approach. *Biomass Bioenergy* 2010;34:1770–9.
- Prasifka JR. Potential biomass reductions to *Miscanthus x giganteus* by stem-boring caterpillars. *J Econ Entomol* 2011;41:1031–42.
- Prasifka JR, Bradshaw JD, Meagher RL, Nagoshi RN, Steffey KL, Gray ME. Development and feeding of fall armyworm on *Miscanthus x giganteus* and switchgrass. *J Econ Entomol* 2009;102:2154–9.
- Prasifka J, Lee DK, Bradshaw J, Parrish A, Gray M. Seed reduction in prairie cordgrass, *Spartina pectinata* link., by the floret-feeding caterpillar *Aethes spartinana*; (Barnes and McDunnough). *Bioenerg Res* 2011;4:1–8.
- Price L, Bullard M, Lyons H, Anthony S, Nixon P. Identifying the yield potential of *Miscanthus x giganteus*: an assessment of the spatial and temporal variability of *M x giganteus* biomass productivity across England and Wales. *Biomass Bioenergy* 2004;26:3–13.
- Raghu S, Spencer JL, Davis AS, Wiedenmann RN. Ecological considerations in the sustainable development of terrestrial biofuel crops. *Curr Opin Environ Sustain* 2011;3:15–23.
- Rawls WJ, Ahuja JR, Brakensiek DL. Estimating soil hydraulic properties from soils data. Workshop on indirect methods for estimating the hydraulic properties of unsaturated soils proceedings. Riverside, CA; 1992. p. 329–41.
- RReDC-NREL. U.S. Solar radiation resource maps: U.S. Solar Radiation Resource Maps: Atlas of the Solar Radiation Data Manual for Flat-Plate and Concentrating Collectors. [http://rredc.nrel.gov/solar/old\\_data/nsrdb/1961-1990/redbook/atlas/](http://rredc.nrel.gov/solar/old_data/nsrdb/1961-1990/redbook/atlas/); 2012.
- Saltelli A, Annoni P. How to avoid a perfunctory sensitivity analysis. *Environ Model Softw* 2010;25:1508–17.
- Sammis TW, Evans DD, Warrick AW. Comparison of methods to estimate deep-percolation rates. *Water Resour Bull* 1982;18:465–70.
- Selfa T, Kulcsar L, Bain C, Goe R, Middendorf G. Biofuels bonanza? Exploring community perceptions of the promises and perils of biofuels production. *Biomass Bioenergy* 2011;35:1379–89.
- Sheppard AW, Raghu S, Begley C, Genovesi P, De Barro P, Tasker A, et al. Biosecurity as an integral part of the new bioeconomy: a path to a more sustainable future. *Curr Opin Environ Sustain* 2011;3:105–11.
- Simmons BA, Loque D, Blanch HW. Next-generation biomass feedstocks for biofuel production. *Genome Biol* 2008;9(242):1–6.
- Spencer JL, Raghu S. Refuge or reservoir? The potential impacts of the biofuel crop *Miscanthus x giganteus* on a major pest of maize. *PLoS ONE* 2009;4:e8336.
- USDA. Biomass crop assistance program. Proposed BCAP giant *Miscanthus (Miscanthus x giganteus)*. United States Department of Agriculture, Farm Service Agency: Establishment and Production in Arkansas, Missouri, Ohio, and Pennsylvania; 2011.
- USDA-NRCS. Web Soil Survey. USDA Natural Resources Conservation Service. <http://websoilsurvey.nrcs.usda.gov/app/WebSoilSurvey.aspx>; 2012.
- Zub HW, Brancourt-Hulmel M. Agronomic and physiological performances of different species of *Miscanthus*, a major energy crop. A review. *Agron Sustain Dev* 2010;30:201–14.